

Driving Flip Origami Motions with Thermal-Responsive Shape Memory Alloy

Yan Zhang¹ and Hongliang Ren^{*1,2}

Abstract—This paper proposes a motion generation approach to flipping origami models. According to the geometrical principle of an infinite flip origami and using the shape memory properties of nickel-titanium alloy with temperature change, the memory alloy spring is selected as the driving units of origami motions. With conductivity, aluminum foil paper is selected as the wire connecting the memory alloy spring. By designing different circuit connection manners, the memory alloy spring will change the temperature deformation and then drive the movement of the origami. The paper provides a detailed description of how to use the geometric principle to design the origami shape, and analyze the movement principle of the model. We use aluminum foil paper and memory alloy spring with serial and parallel circuit design to study the motion form of the combination of origami and memory alloy spring.

Keywords: origami, geometric principle, memory alloy spring.

I. INTRODUCTION

Modern robotics is opening up a new era of robotic intelligence and to meet the need for low-cost manufacturing and mass customization. The design of deformable devices can be found in “printing” robots, pop-up manufacturing techniques and soft sensors like[1][2]. In deployable structures, folding is the primary mechanism for building and articulating, such as how to move the robot through flexible bending [3][4][5]. In particular, the research on bionic robots, soft continuum robots[6], [7], [8], micro-robots pose challenges for driving devices, sensors [9] and models [8] suitable for robot constructions, safety control [10], motion generation, and movement detection [11], [12] [13][14][15][16].

The use of origami to study the model architecture is an economical and fast method due to the inexpensive materials that can be customized on both large scale and small scale [17], [18], [19], [20], [21]. The model design can be uncovered by the mathematical principles hidden behind it. A nickel-titanium (Nitinol) shape memory alloy (SMA) was chosen as the actuator, based on the natural heat dissipation of the memory alloy itself. Nitinol SMA, as a driver for the origami model, is energized to change the

¹Y Zhang and H Ren are with National University of Singapore (Suzhou) Research Institute (NUSRI), Block 1-3, Public Academy, No. 377, Linquan Street, Dushu Lake Science and Education Innovation District, Suzhou Industrial Park, Suzhou, Jiangsu Province, China 215123

²H Ren are with the Department of Biomedical Engineering (BME), National University of Singapore (NUS), Singapore 119077.

*Corresponding author: Hongliang Ren
 hren@ieee.org/ren@nus.edu.sg

This work was supported by NUSRI China Jiangsu Provincial Grant BE2016077 awarded to Dr. Hongliang Ren.

temperature, thereby changing the movement mode of the origami model.

In this paper, an infinitely reversible origami model is designed in combination with a NiTi shape memory alloy spring to study how the origami model can change the temperature by changing its current. The first part of the article introduces how to design the origami model based on the mathematical geometry principle, and analyzes the movement principle of the origami model in detail. The second part of the paper introduces the combination of the origami model and the nickel-titanium shape memory alloy. Attempts to design four different types of segmented circuits, combined with the shape of the inverted origami, are made in serial and parallel experiments, using aluminum foil as the wire. A power-on experiment was performed on the circuit to demonstrate how the origami model moves during power-modulations.

II. ORIGAMI MODELS

A. Origami model concept design

The basic unit of this experiment is the isosceles triangle. Through repeated experiment and comparison, the isosceles triangle with the bottom edge 30mm and the height 30mm is selected as the basic unit of the experiment. The four

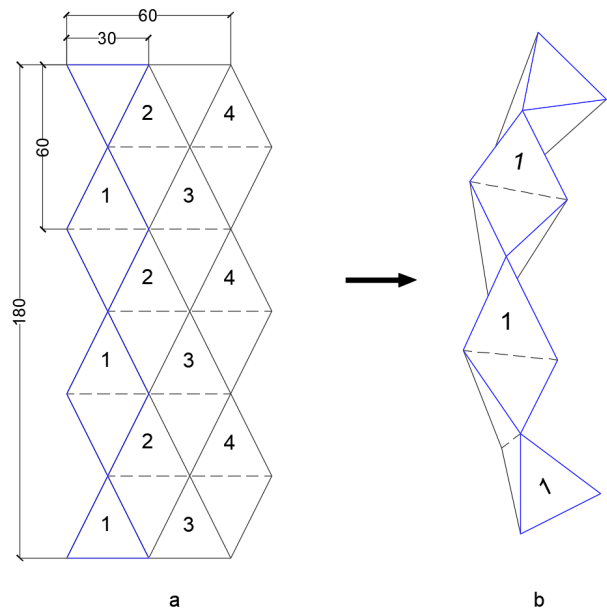


Fig. 1. Origami model design: Figure a crease map, map b renderings.

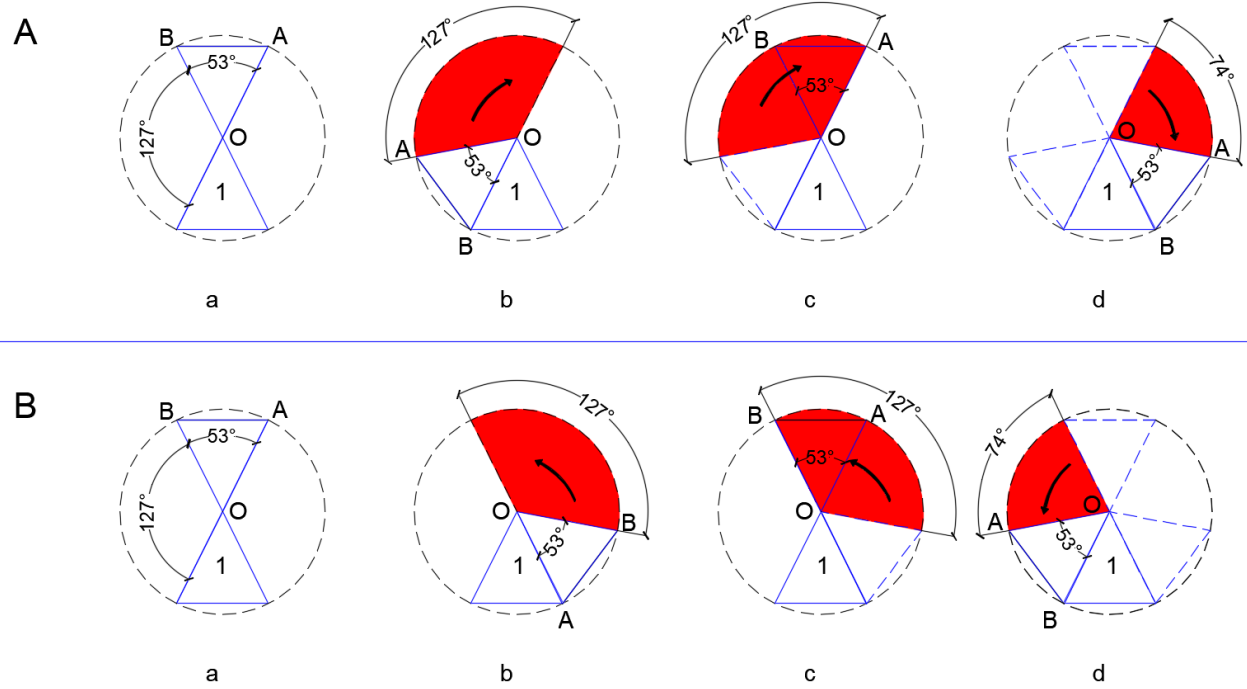


Fig. 2. motion principle:Figure A fixed center O and the following isosceles triangle, ΔABO rotates 201° clockwise; Figure B fixed center O and the underlying isosceles triangle, ΔABO rotates 201° clockwise.

isosceles triangle folds on the same horizontal line can get one tetrahedron. Then choose to draw such an isosceles triangle of 24 basic units, and finally get 6 tetrahedrons, as shown in Fig. 1.

Using AutoCAD automatic computer-aided design software to draw the crease map, in order to facilitate the subsequent experiments, use the numbers 1-4 to advance the number of the figure into 4 reference planes, and the final product is displayed by 6 tetrahedrons, respectively 2 Kind of object, one is a non-closed object, and the other is a closed object, as shown in Fig. 3.

B. The movement principle of the origami model

For the observation of these two kinds of physical origami, the form of motion of the open chain can be variously

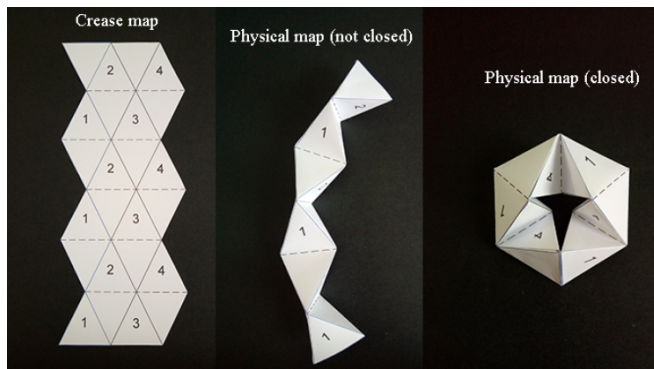


Fig. 3. Physical model.

deformed. Whereas the closed chain has only two modes of motion, inversion, and eversion, and the opposite direction can achieve infinite flipping. Although the movement patterns of the two kinds of objects are very different on the surface, the movement of the most basic units is the same. In order to explore more deformation of the inverted origami, the first uncontained origami is selected as the experimental object in this experiment. Select two connected tetrahedrons as a basic unit, and draw a top view of the basic unit under different motion states, as shown in Fig. 2.

Fig. 2A: Figure a is a top view of a basic motion mode, assuming that the upper isosceles triangle is ΔABO , the intersection of the two isosceles triangles is O, the point O is the center of the circle, the line segment OA is the radius, and an auxiliary circle is drawn. Figure b is the initial state of motion. Fixed center O and the isosceles triangle below (the isosceles triangle labeled as number 1 in the figure), one edge OB of ΔABO abuts the side length of the left side of the isosceles triangle below, make the two coincide at the initial state of the movement. Then, ΔABO is rotated clockwise along the center O, and its motion state is as shown in Fig. c and finally becomes graph d. In this movement, the line segment OA is rotated clockwise around the center O by 201° (shown by a red fan in the figure).

Fig. 2B: The motion pattern is similar to that of Figure A except that the direction is opposite. Assume that Figure b is the initial state of motion, ΔABO rotates counterclockwise along the center O, and its motion state is shown in Fig. c and Fig. d. The line segment OB is rotated counterclockwise by 201° around the center O (shown by a red fan in the figure).

Although only the difference in the direction of rotation is shown in the top view, there may be variations in how much in actual motion.

III. SMA-DRIVEN ORIGAMI DESIGN

A. The principle of motion generation using shape memory alloy

In the model of flipping the origami, two connected tetrahedrons are selected as the basic unit of the experiment, and the memory alloy spring is fixed in the middle of the two tetrahedrons, because the aluminum foil paper has electrical conductivity, relatively high melting point, and is not easily damaged after heating. Therefore, aluminum foil paper is used instead of the wire to fix the two ends of the spring, and then the positive and negative poles of the power supply are connected, the memory alloy spring is energized, the temperature rises after energization, and the memory alloy spring returns from the stretched state to the initial contracted state and the origami is deformed, as shown in Fig. 4.

B. Segmented circuit design of shape memory alloy

The inverted origami model is composed of 6 identical tetrahedrons, divided into four faces, using four segments of the same shape memory alloy spring (wire diameter 0.5 mm, diameter 3.2 mm, tight compression 10 mm, temperature 80°C), Origami performs different circuit designs.

Stage I experiment: a memory alloy spring working with a basic unit of origami.

Section II experiment: two basic memory alloy springs and two basic unit combinations of origami.

Stage III experiment: three-section memory alloy spring and three basic unit combinations of origami.

Stage IV experiment: four-section memory alloy spring and origami four basic unit combination.

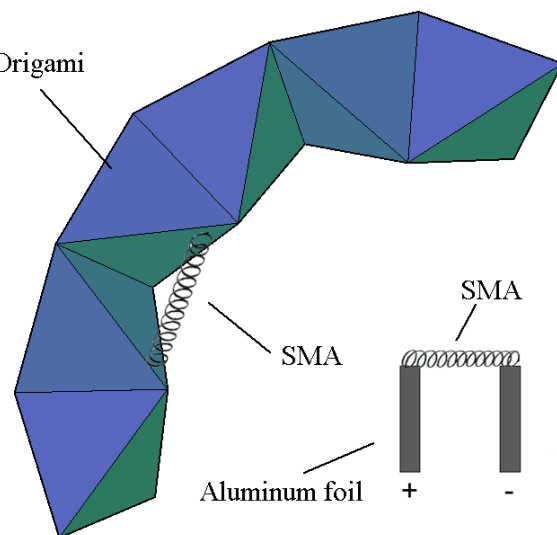


Fig. 4. 3D rendering of the origami model.

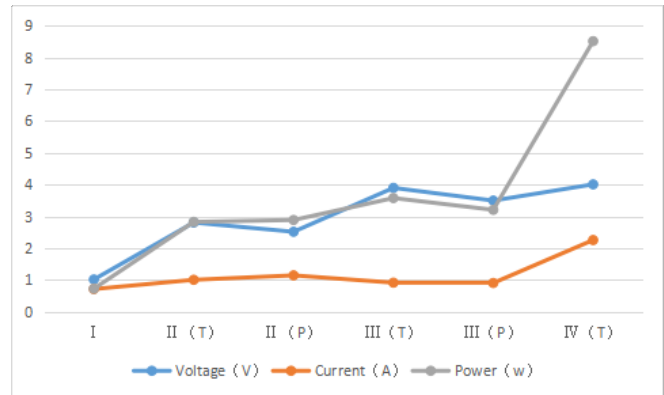


Fig. 5. Segmented electric power.

Fig. 5 shows the final current, voltage and power values required for each segmentation motion. It can be seen that the resistance of the spring and the foil paper is almost negligible, basically satisfying the power formula:

$$P = UI$$

Table 1, the number of memory alloy spring connection circuit methods are divided into serial and parallel, combined with the characteristics of the flip origami model, in which the circuit design of the II segment experiment and the III segment experiment were respectively performed in sequences and parallel experiments, The IV segment is designed as a parallel circuit, and the I segment is an independent experiment. The circled numbers in the table correspond to the order of movement of the alloy springs after energization, the symbol “|” is the initial stretch state, and the symbol “>” is the final compression tight state.

TABLE I
CIRCUIT DESIGN OF SEGMENTED SMA DRIVE ORIGAMI.

Quantity	Circuit	1	2	3	4	5
I			>			
II	Tandem		>			
	Tandem		>			
III	in parallel		>			
	in parallel			>		
IV	Tandem		>			
	Tandem		>		>	

C. SMA driven origami I segment experiment

Fig. 6 is a stage I experiment: select the first surface (marked by the number 1 in Fig. 6a) to fix a piece of memory alloy spring, connect a small piece of aluminum foil paper at both ends, and fold the origami, as shown in Fig. 6b, Fig. 6b

“ | ” represents the memory alloy spring at the initial state of stretching at room temperature, using aluminum foil instead of the wire to connect the positive and negative poles of the power supply, adjust the voltage, the temperature rises, the spring begins to shrink to a tight state as Fig. 6 c, the “ > ” of Figure c represents After the memory alloy spring is energized, the temperature exceeds 80°C and shrinks to a tight state, which drives the origami to flip.

D. SMA driven origami II segment experiment

Fig. 7 is a II-stage experiment (series circuit): select the first surface (marked by the number 1 in Figure a) to fix the two-section memory alloy spring, use aluminum foil paper as a series circuit, fold the origami, as shown in Figure b, two “ | ” mean that the SMA has been stretched at room temperature as an initial state and connected in series. Replace the wire with the aluminum foil to connect the positive and negative poles of the power supply, adjust the voltage, increase the temperature, and the spring shrinks to a tight state as shown in Fig. 7 c. The two “ > ” indicate that the temperature of the SMA exceeds 80°C and begins to shrink to a tight state. At the same time, the origami flip changes.

Fig. 8 is a II-stage experiment (parallel circuit): two faces (marked by numbers 1 and 2 in Figure a) are selected to fix the two-section memory alloy spring, and the aluminum foil is used for the loop, and the folded origami is shown in Figure b, two “ | ” represent the SMA to stretch the initial state at room temperature and connect in parallel. We replace the wire with the aluminum foil to connect the positive and negative poles of the power supply, adjust the voltage, increase the temperature, and the spring begins to contract. We let the shape change first. The “ > ” represents SMA first shrinks to a tight state, and then the Fig. 8d deformation, which drives the origami to change in turn.

E. SMA driven origami III segment experiment

Fig. 9 is a III-stage experiment (series circuit): Select the second surface (marked by the number 2 in Figure a) to fix the three-section memory alloy spring, use aluminum foil paper as a series circuit, fold the origami, as shown in

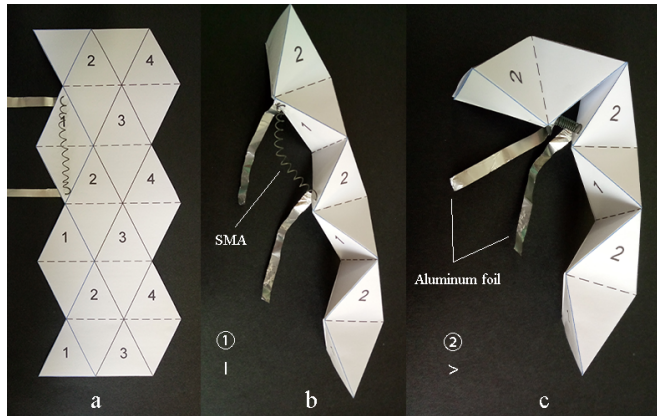


Fig. 6. Stage I experiment.

Figure b, three “ | ” stand for SMA to stretch the initial state at room temperature and make a series connection. We replace the wire with the aluminum foil to connect the positive and negative poles of the power supply, adjust the voltage, increase the temperature, and the spring shrinks to a tight state as shown in Fig. 9 c. The three “ > ” indicate that the temperature of the SMA exceeds 80°C, while driving origami flip changes.

Fig. 10 is a III-stage experiment (parallel circuit): three faces (marked by numbers 1 and 2 and 3 in Figure a) are

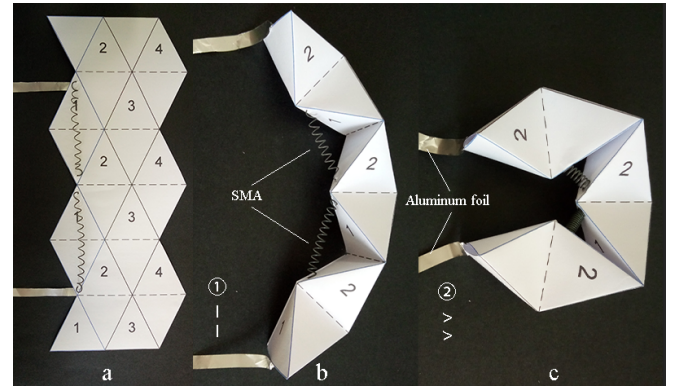


Fig. 7. Stage II experiment (series circuit).

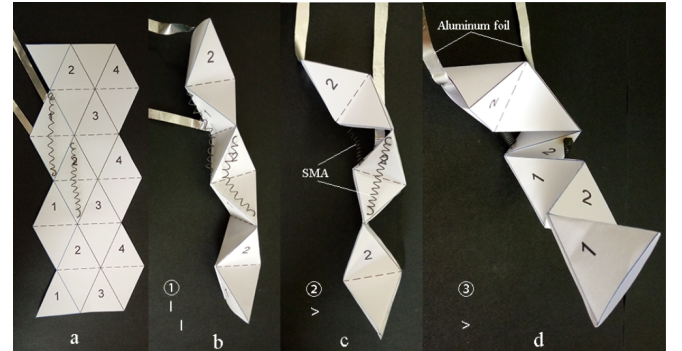


Fig. 8. Stage II experiment (parallel circuit).

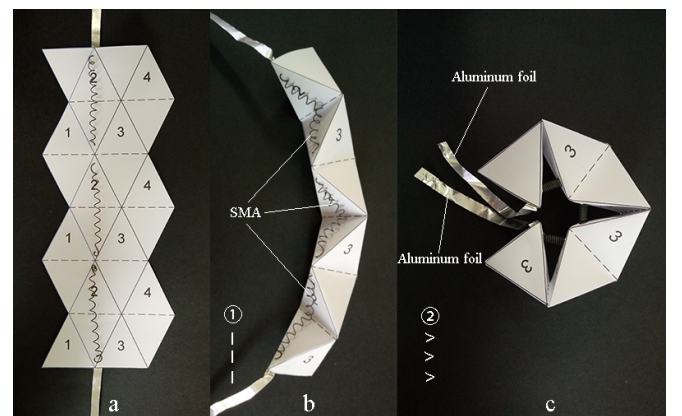


Fig. 9. Stage III experiment (series circuit).

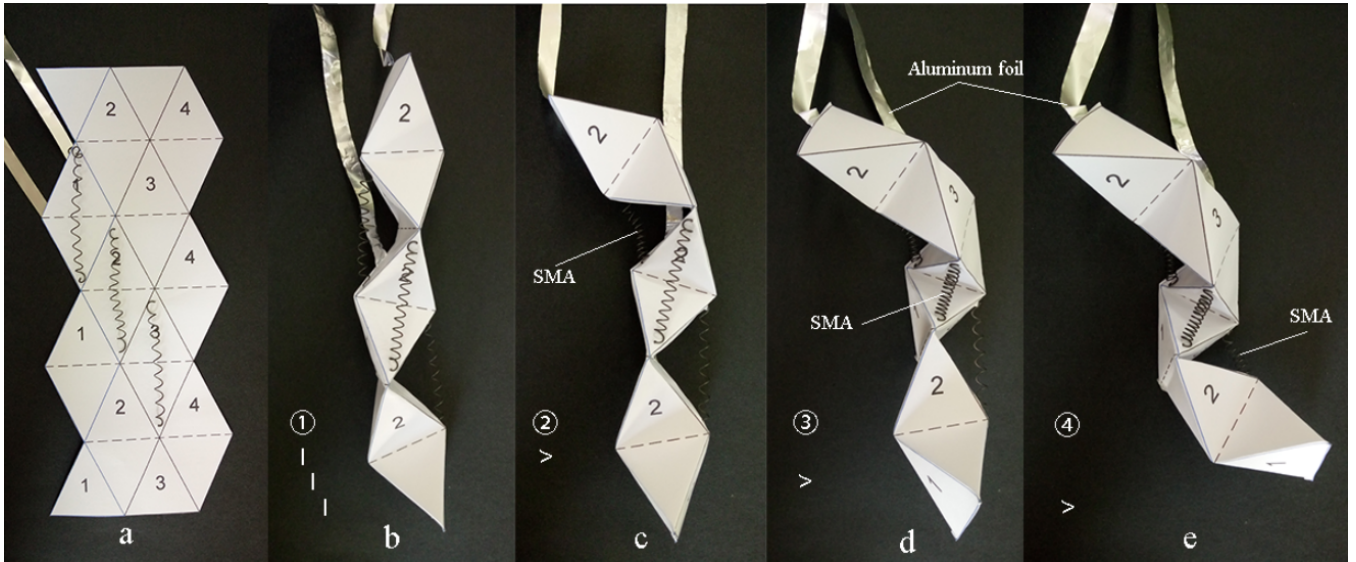


Fig. 10. Stage III experiment (parallel circuit).

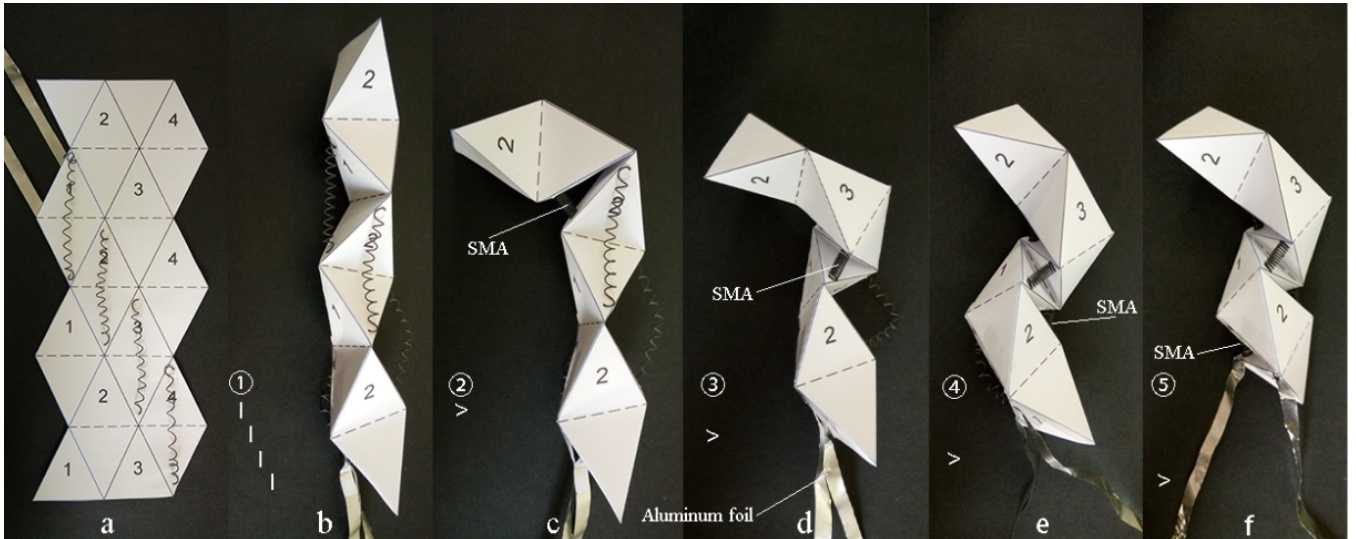


Fig. 11. Stage IV experiment (parallel circuit).

selected to fix the two-section memory alloy spring, and the aluminum foil is used for the loop, and the folded origami is shown in Fig. 10b, three “|” stand for SMA to stretch the initial state at room temperature and make a parallel connection. We turn on the positive and negative poles of the power supply, adjust the voltage, the temperature of the alloy spring starts to shrink, and finally compress into a tight spring, and then perform the contraction motion in sequence. First, the c-shaped change is made. The “>” represents the memory alloy spring first shrinks and forms a section. Tight spring, then d-shaped deformation, “>” represents the memory alloy spring to shrink and form a tight spring, and finally make a Fig. 10 e, “>” represents SMA finally shrinks into a tight spring, which drives the origami to fold in turn.

F. SMA driven origami IV segment experiment

Fig. 11 is the IV segment experiment (parallel circuit) of the inverted origami model: the first side of the selected origami (marked by the number 1 in Figure a), the second side (marked by the number 2 in Figure a), the third The surface (marked by the number 3 in Figure a), the fourth surface (marked by the number 4 in Figure a) fixes the four-section memory alloy spring forming a parallel circuit. The crease folds the origami, as shown in Figure b, the four “|” stand for SMA to stretch the initial static state at room temperature and make a parallel connection, turn on the positive and negative poles of the power supply, adjust the voltage, and the temperature of the alloy spring rises. After shrinking and finally compressing into a tight spring, the contraction movement makes a c-shaped deformation. The

symbol “>” indicates that the SMA first shrinks to a tight spring, as shown in Figure c, and then changes to Fig. d, Fig. e and Fig. f, shrinking to a tight state and driving the fold flip order.

IV. CONCLUSIONS

It can be seen from the above examples that from the perspective of exploration, this paper mainly discusses the geometrical mathematical principle of origami, designs the origami model, studies the motion generation principle of flipping origami with shape memory alloy to flip the origami. We designed four different types of segmented circuit design, combined with the shape of flipping origami, and made series and parallel experiments respectively. Using aluminum foil paper as the wire, the circuit was energized to observe the movement mode of the alloy spring. In the series circuit model, the alloy spring is almost simultaneously contracted, and finally forms the original tight compression state, and at the same time drives the movement of the inverted origami. In the parallel circuit model, the alloy springs are sequentially performed. Movement, the alloy wire away from the power end is the first movement, and the alloy spring near the power end is the last movement. Considering that this topic is only an initial exploratory research topic, there are still many unpublished contents in the text, which can only be improved on the basis of experiments in the future. As an exploratory research topic, it has the following aspects to be further improved:

- Improve the specific structural design of the memory alloy spring, because the tight spring itself has a certain length, the flipping origami cannot be completely or tightly deformed, and it is still necessary to construct a driver with more perfect functions to continuously provide kinetic energy.
- Select the appropriate alloy spring, combined with the closed origami model, to study the possibility of infinite flipping.

ACKNOWLEDGMENT

This work was supported by NUSRI China Jiangsu Provincial Grant BE2016077 awarded to Dr. Hongliang Ren. We would like to thank Tingchen Liao for his enthusiastic help.

REFERENCES

- [1] K. S. Kumar, H. Ren, and Y. H. Chan, “Soft tactile sensors for rehabilitation robotic hand with 3d printed folds,” in *International Conference for Innovation in Biomedical Engineering and Life Sciences ICIBEL2017*. Springer, 2017, pp. 55–60.
- [2] C. Shi, X. Luo, P. Qi, T. Li, S. Song, Z. Najdovski, T. Fukuda, and H. Ren, “Shape sensing techniques for continuum robots in minimally invasive surgery: A survey,” *IEEE Transactions on Biomedical Engineering*, vol. 64, no. 8, pp. 1665–1678, aug 2017.
- [3] A. V. Prituja, H. Banerjee, and H. Ren, “Electromagnetically enhanced soft & flexible bend sensor: A quantitative analysis with different cores, in press,” *IEEE Sensors Journal*, vol. 18, no. 9, pp. 3580–3589, may 2018.
- [4] S. K. Kirthika, G. P. J. Vedhagiri, and H. Ren, “Fabrication and comparative study on sensing characteristics of soft textile-layered tactile sensors,” *IEEE Sensors Letters*, vol. 1, no. 3, pp. 1–4, 2017.
- [5] G. Ponraj, S. K. Kirthika, N. V. Thakor, C.-H. Yeow, S. L. Kukreja, and H. Ren, “Development of flexible fabric based tactile sensor for closed loop control of soft robotic actuator,” in *CASE17, IEEE International Conference on Automation Science and Engineering*, Sep. 2017, pp. 678–685.
- [6] Z. Li, L. Wu, H. Yu, and H. Ren, “Kinematic comparison of surgical tendon-driven manipulators and concentric tube manipulators,” *Mechanism and Machine Theory*, vol. 107, pp. 148–165, 2017. [Online]. Available: <http://www.sciencedirect.com/science/article/pii/S0094114X16302580>
- [7] Y. Sun, S. Song, X. Liang, and H. Ren, “A miniature soft robotic manipulator based on novel fabrication methods,” *IEEE Robotics and Automation Letters*, vol. 1, no. 2, pp. 617–623, July 2016.
- [8] L. Wu, X. Yang, K. Chen, and H. Ren, “A minimal poe-based model for robotic kinematic calibration with only position measurements,” *IEEE Transactions on Automation Science and Engineering*, vol. 12, no. 2, pp. 758–763, 2015.
- [9] S. Song, Z. Li, H. Ren, and H. Yu, “Shape reconstruction for wire-driven flexible robots based on bezier curve and electromagnetic positioning,” *Mechatronics*, vol. 29, no. 99, pp. 28 – 35, 2015. [Online]. Available: <http://www.sciencedirect.com/science/article/pii/S0957415815000689>
- [10] H. Ren and M. Q.-H. Meng, “Rate control to reduce bioeffects in wireless biomedical sensor networks,” in *3rd Annual International Conference on Mobile and Ubiquitous Systems - Workshops*, July 2006, pp. 1–7.
- [11] C. Nadeau, H. Ren, A. Krupa, and P. E. Dupont, “Intensity-based visual servoing for instrument and tissue tracking in 3d ultrasound volumes,” *IEEE Transactions on Automation Science and Engineering*, vol. 12, no. 1, pp. 367–371, jan 2015.
- [12] H. Ren, N. V. Vasilyev, and P. E. Dupont, “Detection of curved robots using 3d ultrasound,” in *IROS 2011, IEEE/RSJ International Conference on Intelligent Robots and Systems*, 2011, pp. 2083–2089.
- [13] Godwin and H. Ren, “Estimation of object orientation using conductive ink and fabric based multilayered tactile sensor,” in *ICRA2018, IEEE International Conference on Robotics and Automation*, 31 May, 2018, pp. 2907–2912.
- [14] T. Li, C. Shi, Y. Tan, R. Li, Z. Zhou, and H. Ren, “A diaphragm type fiber bragg grating vibration sensor based on transverse property of optical fiber with temperature compensation,” *IEEE Sensors Journal*, vol. 17, no. 4, pp. 1021 – 1029, 2017.
- [15] H.-K. Kim, S. Lee, and K.-S. Yun, “Capacitive tactile sensor array for touch screen application,” *Sensors and Actuators A: Physical*, vol. 165, no. 1, pp. 2–7, 2011.
- [16] S. J. Kim, H. Moon, H. R. Choi, and J. C. Koo, “Development of a slip sensor using separable bilayer with ecoflex-nbr film,” in *Sensors and Smart Structures Technologies for Civil, Mechanical, and Aerospace Systems 2017*, vol. 10168. International Society for Optics and Photonics, 2017, p. 1016835.
- [17] A. J. Taylor, T. Slutsky, L. Feuerman, H. Ren, J. Tokuda, K. Nilsson, and Z. T. H. Tse, “Mr conditional sma-based origami joint,” *IEEE/ASME Transactions on Mechatronics*, pp. 1–1, 2019.
- [18] H. Banerjee, N. Pusalkar, and H. Ren, “Single-motor controlled tendon driven peristaltic soft origami robot,” *Journal of Mechanisms and Robotics*, vol. 10, no. 6, p. 064501, sep 2018.
- [19] ———, “Preliminary design and performance test of tendon-driven origami-inspired soft peristaltic robot,” in *ROBIO 2015, IEEE International Conference on Robotics and Biomimetics*. IEEE, Dec. 2018, pp. –.
- [20] A. R. Deshpande, Z. T. H. Tse, and H. Ren, “Origami-inspired bi-directional soft pneumatic actuator with integrated variable stiffness mechanism,” in *2017 18th International Conference on Advanced Robotics (ICAR)*, July 2017, pp. 417–421.
- [21] M. Johnson, Y. Chen, S. Hovet, S. Xu, B. Wood, H. Ren, J. Tokuda, and Z. T. H. Tse, “Fabricating biomedical origami: a state-of-the-art review,” *International Journal of Computer Assisted Radiology and Surgery*, vol. 12, pp. 2023–2032, 2017. [Online]. Available: <http://dx.doi.org/10.1007/s11548-017-1545-1>